Molecular Therapy
Methods & Clinical Development
Original Article

AAV-Mediated ApoC2 Gene Therapy: Reversal of Severe Hypertriglyceridemia and Rescue of Neonatal Death in ApoC2-Deficient Hamsters

Chun Yang,[1] Wenhong Tian,[2] Sisi Ma,[2] Mengmeng Guo,[1] Xiao Lin,[1] Fengying Gao,[1] Xiaoyan Dong,[2] Mingming Gao,[3] Yuhui Wang,[1] George Liu,[1] and Xunde Xian[1,4]

[1]Institute of Cardiovascular Sciences and Key Laboratory of Molecular Cardiovascular Sciences, Ministry of Education, Peking University, Beijing 100191, China; [2]Beijing FivePlus Molecular Medicine Institute Co. Ltd., Beijing 100176, China; [3]Laboratory of Lipid Metabolism, Institute of Basic Medicine, Hebei Medical University, Shijiazhuang 050017, China

Apolipoprotein C2 (ApoC2) is a key activator of lipoprotein lipase for plasma triglyceride metabolism. ApoC2-deficient patients present with severe hypertriglyceridemia and recurrent acute pancreatitis, for whom the only effective treatment is the infusion of normal plasma containing ApoC2. However, since ApoC2 has a fast catabolic rate, a repeated infusion is required, which limits its clinical use. To explore a safe and efficient approach for ApoC2 deficiency, we herein established an adeno-associated virus expressing human ApoC2 (AAV-hApoC2) to evaluate the efficacy and safety of gene therapy in ApoC2-deficient hypertriglyceridemic hamsters. Administration of AAV-hApoC2 via jugular or orbital vein in adult and neonatal ApoC2-deficient hamsters, respectively, could prevent the neonatal death and effectively improve severe hypertriglyceridemia of ApoC2-deficient hamsters without side effects in a long-term manner. Our novel findings in the present study demonstrate that AAV-hApoC2-mediated gene therapy will be a promising therapeutic approach for clinical patients with severe hypertriglyceridemia caused by ApoC2 deficiency.

INTRODUCTION

Lipoprotein lipase (LPL) complexes hydrolyze endogenous and exogenous triglycerides (TGs) carried in very-low-density lipoprotein (VLDL) and chylomicron (CM) in plasma, respectively. The released free fatty acids (FFAs) are taken up by adipocytes to form TGs for storage or utilized as energy in skeletal muscle and myocardium. Many key proteins, including apolipoprotein Cs (ApoCs), angiopoietin-like proteins (ANGPTLs), and GPIHBP1, can regulate LPL activity through various posttranslational regulatory mechanisms,[1,2] in which ApoC2 is an essential activator of LPL activity[3,4] and plays a crucial role in LPL-mediated TG hydrolysis.[5,6]

Hypertriglyceridemia (HTG) is a multifactorial disorder with genetic and secondary forms, characterized by abnormal synthesis or impaired degradation of TGs, leading to excess TGs accumulated in plasma. Familial chylomicronemia syndrome (FCS) primarily caused by loss-of-function mutations in LPL is a group of extremely rare monogenic conditions with a reported prevalence of about one in 1 million.[7,8]

In addition, note that ApoC2 deficiency is also one of the most common causes of FCS with severe HTG (sHTG) and recurrent HTG-induced acute pancreatitis (HTAP), which can be life-threatening.[9–13] There are a total of 30 different ApoC2 mutant cases being reported in different populations worldwide,[8] suggesting that ApoC2 deficiency also requires attention.

To date, many kinds of gene-modified mouse models have been successfully generated and widely used in the study of human lipid metabolism disorders. Unfortunately, it has been reported that ApoC2 deletion due to a frameshift caused embryonic lethality in mice,[14] and the only viable mouse model carrying ApoC2 mutants was developed, showing an excess of immature ApoC2 in plasma and moderate HTG, which substantially differs from clinical ApoC2-deficient patients, indicating that it is not a true ApoC2-deficient animal model.[14] Recently, an ApoC2-deficient zebrafish model with sHTG was created to study ApoC2 function,[15] but because of the differences in lipid profile and low homogeneity of the *Apoc2* gene between zebrafish and humans, the further application and practical value of the ApoC2-deficient zebrafish model are limited.

Based on the advanced characteristics of Syrian golden hamsters that are similar to humans in lipid metabolism, our laboratory applied CRISPR-Cas9 technology to establish hamster models lacking some

Received 20 March 2020; accepted 10 July 2020;
https://doi.org/10.1016/j.omtm.2020.07.011.

[4]Lead contact

Correspondence: Xunde Xian, Institute of Cardiovascular Sciences and Key Laboratory of Molecular Cardiovascular Sciences, Ministry of Education, Peking University, Beijing 100191, China.
E-mail: xianxunde@bjmu.edu.cn
Correspondence: George Liu, Institute of Cardiovascular Sciences and Key Laboratory of Molecular Cardiovascular Sciences, Ministry of Education, Peking University, Beijing 100191, China.
E-mail: georgeliu@bjmu.edu.cn

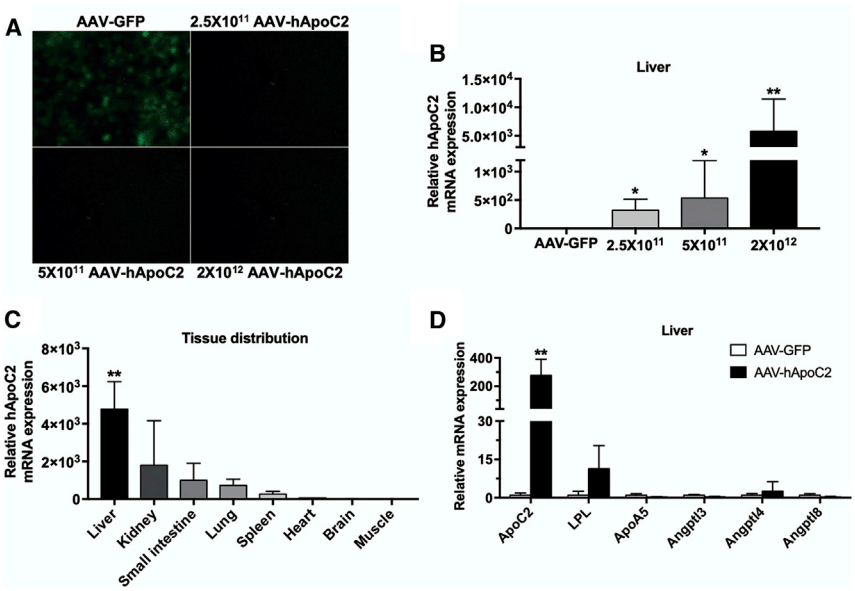

Figure 1. The Expression Pattern of hApoC2 and Other TG Metabolism-Related Genes in Adult ApoC2$^{-/-}$ Hamsters Treated with AAV-hApoC2

(A) Representative images of cryosections of liver from adult ApoC2$^{-/-}$ hamsters treated with AAV-GFP or AAV-hApoC2. Adult ApoC2$^{-/-}$ hamsters were administered 2 × 10^{12} vg of AAV-GFP or AAV-hApoC2 at 2.5 × 10^{11}, 5 × 10^{11}, or 2 × 10^{12} vg. The green fluorescence of liver was analyzed at week 8 after AAV injection. (B) Quantitative analysis of hepatic hApoC2 mRNA expression relative to GAPDH in animals described in A. N = 3 per group. *p < 0.05, **p < 0.01. (C) Tissue distribution of hApoC2 expression in adult ApoC2$^{-/-}$ hamsters injected with AAV-hApoC2. Quantitative analysis of hApoC2 mRNA expression was performed in liver, kidney, small intestine, lung, spleen, heart, and muscle in AAV-hApoC2-treated adult ApoC2$^{-/-}$ hamsters at a dose of 2 × 10^{12} vg. N = 3 per group, **p < 0.01. (D) Quantitative analysis of mRNA expression of genes regulating hepatic TG metabolism. The hepatic mRNA expression levels of LPL, ApoA5, Angptl3, Angptl4, and Angptl8 at week 8 were analyzed by real-time PCR in adult ApoC2$^{-/-}$ hamsters injected with AAV-hApoC2 at a dose of 2 × 10^{12} vg. N = 3 per group. **p < 0.01.

key genes regulating lipid metabolism, including the LDL receptor and lecithin-cholesterol acyltransferase (LCAT).[16,17] In our previous study, ApoC2 knockout hamsters created by the CRISPR-CAS9 system showed neonatal death secondary to sHTG, which could be rescued by continuous intravenous (i.v.) infusion of wild-type (WT) hamster serum and then survival to adulthood with sHTG, thus providing an ideal animal model for the study of sHTG caused by ApoC2 deficiency.[18]

To our knowledge, clinical treatment for patients with ApoC2 deficiency has not yet been systemically reported, and conventional lipid-lowering drugs are largely ineffective. Transfusion of normal plasma containing ApoC2 may only be applied to save lives during the onset of severe pancreatitis.[15,19] Moreover, results from experimental animals showed that injection of the ApoC2 mimetic peptide into ApoC2 mutant mice normalized TG levels.[14] However, ApoC2 from normal plasma and ApoC2 mimetic peptide are metabolized rapidly in circulation, limiting their clinical use because frequent inputs are required to correct sHTG for a lifetime. Thus, gene replacement therapy could be an optimal regimen for ApoC2-deficienct patients with this well-defined etiology. Recently, adeno-associated virus (AAV) has been reported to be an ideal vector used successfully for gene therapy in different human diseases.[20–22]

Therefore, in the present study we aimed to use ApoC2 knockout hamsters to investigate the efficacy and safety of AAV-mediated ApoC2 gene therapy, and provide a potential therapeutic approach for severe hypertriglyceridemic patients with ApoC2 deficiency.

RESULTS

Complete Correction of sHTG in Adult ApoC2$^{-/-}$ Hamsters

First, we investigated whether the liver could be efficiently infected by the AAV construct *in vivo*. AAV-GFP was injected into adult ApoC2$^{-/-}$ hamsters through the jugular vein and green fluorescence was observed in the liver, indicating a successful AAV-mediated GFP expression (Figure 1A). Then, AAV expressing human ApoC2 (AAV-hApoC2) with different doses at 2.5 × 10^{11} vector genomes (vg) (low), 5 × 10^{11} vg, (medium) and 2 × 10^{12} vg (high) was also injected i.v. into adult ApoC2$^{-/-}$ hamsters. The results showed that the mRNA expression level of hApoC2 in the liver was significantly higher than that in the control group in a dose-dependent manner (Figure 1B). In the meantime, we also found that hApoC2 was expressed in other organs, including kidney, small intestine, and lung by 30%, 20%, and 20%, respectively, when compared to liver. However, there was no hApoC2 detected in spleen, heart, and skeletal muscle (Figure 1C). Furthermore, to study whether the restoration of ApoC2 expression in knockout hamsters could influence other genes involved in TG metabolism in liver, we measured the mRNA expression of LPL and its regulators, such as ApoA5, Angptl3, Angptl4, and Angptl8, but no changes were observed (Figure 1D).

Next, in order to investigate whether treatment with AAV-hApoC2 at different doses could efficiently correct HTG in adult ApoC2$^{-/-}$ hamsters, plasma concentrations of TGs and total cholesterol (TC) were measured before and 8 weeks after administration of AAV-hApoC2. As shown in Figure 2A, the milky plasmas of sHTG in ApoC2$^{-/-}$ hamsters were completely normalized to a clear appearance by high-dose AAV-hApoC2 (2 × 10^{12} vg) at week 8 (W8). In comparison with AAV-GFP-treated animals, TG levels were significantly reduced by 85%, 93%, and 97% in the groups receiving low, medium, and high doses of AAV-hApoC2, respectively, which are comparable to WT hamsters with TGs at 210.9 ± 16.17 mg/dL (Figure 2B). TC levels, alternatively, were all markedly decreased by 60% without significant difference among the three AAV-hApoC2-treated groups (Figure 2B). Furthermore, hApoC2 was detected in plasma in all three treated groups as well (Figure 2C). To observe the time

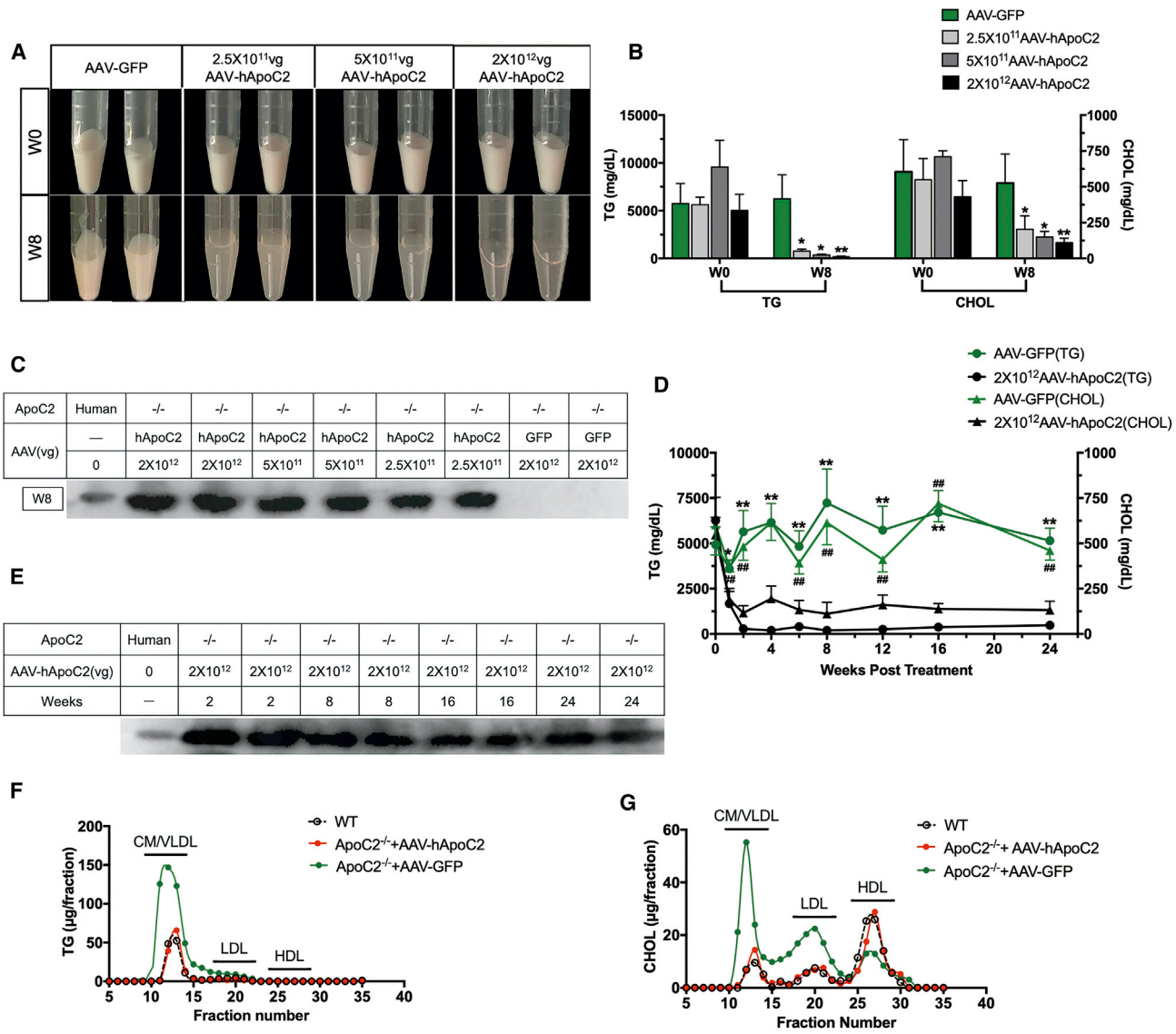

Figure 2. Effects of AAV-Mediated hApoC2 Expression on Plasma Lipids and Lipoproteins in Adult ApoC2$^{-/-}$ Hamsters

(A) Representative photos of plasma samples from adult ApoC2$^{-/-}$ hamsters before (W0) and 8 weeks (8W) after treatment with AAV-hApoC2 at three doses of 2.5×10^{11}, 5×10^{11}, and 2×10^{12} vg; the AAV-GFP-treated group at a dose of 2×10^{12} vg was used as control. (B) Analysis of plasma TG and cholesterol (CHOL) levels in animals from A. N = 3–4 per group. *$p < 0.05$, **$p < 0.01$. (C) Representative western blots of plasma hApoC2 protein at week 8 (W8) after administration of AAV-hApoC2 at three doses of 2.5×10^{11}, 5×10^{11}, and 2×10^{12} vg. (D) Time-course analysis of TG and CHOL levels in AAV-GFP- or AAV-hApoC2-treated adult ApoC2$^{-/-}$ hamsters with a dose of 2×10^{12} vg. N = 4–6 per group. *$p < 0.05$, **$p < 0.01$. (E) Representative western blots of plasma hApoC2 protein in adult ApoC2$^{-/-}$ hamsters at weeks 2, 8, 16, and 24 after administration of AAV-hApoC2 at a dose of 2×10^{12} vg. (F) FPLC analysis of TG distribution from pooled plasma in WT, AAV-GFP-, and AAV-hApoC2-treated adult ApoC2$^{-/-}$ hamsters with a dose of 2×10^{12} vg at week 8. N = 6–8 per group. (G) FPLC analysis of CHOL distribution from pooled plasma in WT, AAV-GFP-, and AAV-hApoC2-treated adult ApoC2$^{-/-}$ hamsters with a dose of 2×10^{12} vg at week 8. N = 6–8 per group.

course of AAV-mediated gene therapy, we chose the high dose for the purposes of our experiment. It was shown that after AAV-hApoC2 administration, the lipid-lowering effects on TGs and TC were observed at week 1 and maintained at the same low levels until the endpoint at week 24, ensuring the achievement of a long-term expression of hApoC2 (Figure 2D). Similarly, hApoC2 in the plasma could be detected at the indicated time points during the 24-week experimental period (Figure 2E).

Moreover, the plasma lipoprotein profile in ApoC2$^{-/-}$ hamsters was greatly improved by AAV-hApoC2 administration. As shown in Figures 2F and 2G, Fast protein liquid chromatography (FPLC)

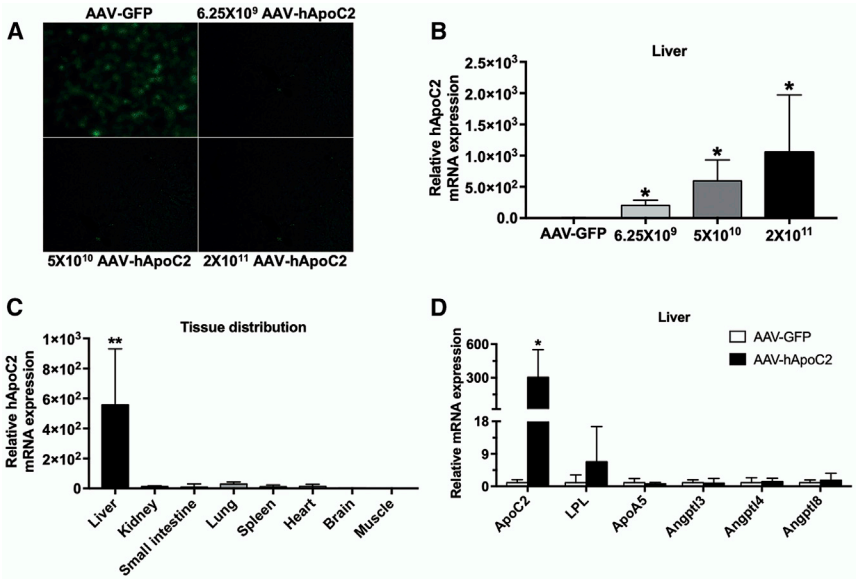

Figure 3. The Expression Pattern of ApoC2 and Other TG Metabolism-Related Genes in Neonatal ApoC2$^{-/-}$ Hamsters Treated with AAV-hApoC2 via Orbital Vein

(A) Representative images of cryosections of liver from neonatal ApoC2$^{-/-}$ hamsters treated with AAV-GFP or AAV-hApoC2. Neonatal ApoC2$^{-/-}$ hamsters were administered with 2×10^{11} vg of AAV-GFP or AAV-hApoC2 at 6.25×10^{9}, 5×10^{10}, or 2×10^{11} vg. The green fluorescence of liver was analyzed at the week 8 after AAV injection. (B) Quantitative analysis of hepatic hApoC2 mRNA expression relative to GAPDH in animals described in A. N = 3 per group. *$p < 0.05$. (C) Tissue distribution of hApoC2 expression in neonatal ApoC2$^{-/-}$ hamsters injected with AAV-hApoC2. Quantitative analysis of hApoC2 mRNA expression was performed in liver, kidney, small intestine, lung, spleen, heart, and muscle in AAV-hApoC2-treated neonatal ApoC2$^{-/-}$ hamsters at a dose of 2×10^{11} vg. N = 3 per group. **$p < 0.01$. (D) Quantitative analysis of mRNA expression of genes regulating hepatic TG metabolism. The hepatic mRNA expression levels of LPL, ApoA5, Angptl3, Angptl4, and Angptl8 at week 8 were analyzed by real-time PCR in neonatal ApoC2$^{-/-}$ hamsters injected with AAV-hApoC2 at a dose of 2×10^{11} vg. N = 3 per group. *$p < 0.05$.

analysis of the plasma from ApoC2$^{-/-}$ hamsters demonstrated a huge peak of both TGs and cholesterol in VLDL/CM fractions, while cholesterol in the LDL fraction was greatly increased, but it was reduced by nearly 50% in the high-density lipoprotein (HDL) fraction, as compared with WT hamsters. However, after AAV-hApoC2 administration, the abnormal distribution of plasma lipoproteins in ApoC2$^{-/-}$ hamsters was corrected completely. The amount of TGs in VLDL/CM was markedly decreased, and cholesterol in LDL was also reduced, whereas HDL cholesterol was increased to the similar extent as that observed in WT hamsters.

Prevention of Death and sHTG in Neonatal ApoC2$^{-/-}$ Hamsters

Since ApoC2 deficiency is diagnosed as early as infancy, we then explored the feasibility of AAV delivery to the neonatal hamsters. We first sought to administer the AAV-GFP to newborn ApoC2$^{-/-}$ pups via the orbital vein. The cryosections of liver from these pups 7 days afterward showed green fluorescence, indicating that AAV successfully mediated GFP gene expression in the liver (Figure 3A). We then injected AAV-hApoC2 with different doses to these pups via a similar route on day 3 after birth. To our surprise, all neonatal ApoC2$^{-/-}$ hamsters survived to week 8. Levels of hApoC2 mRNA were increased dose-dependently in the liver (Figure 3B). The expression pattern of hApoC2 in various tissues in the pups was slightly different from that of adult animals receiving AAV-hApoC2. The liver showed the highest expression level of hApoC2 mRNA, while the kidneys, small intestine, lungs, spleen, heart, and muscle presented virtually undetectable levels (Figure 3C). Analysis of the genes related to TG metabolism in the liver after AAV-hApoC2 administration demonstrated no significant changes in LPL, ApoA5, Angptl3, Angptl4, and Angptl8, except for a significant increase in hApoC2 (Figure 3D).

In experiments with neonatal hamsters the proper controls cannot be designed as in the experiments for adults because ApoC2$^{-/-}$ hamster pups died in the neonatal period. Therefore, AAV-GFP-injected hamsters serving as controls received daily orbital vein infusion of WT hamster serum from day 3 of birth until weaning, which resulted in near normal TG levels of 210.9 ± 16.17 mg/dL shown in WT hamsters. However, the plasma TG concentration was increased to 7,000–8,000 mg/dL after termination of serum infusion. The comparison of AAV-hApoC2 treated with AAV-GFP was begun then. It was found that to different extents, the milky plasma was corrected (Figure 4A), and plasma TG levels were significantly reduced in a dose-dependent manner at week 8 after AAV-hApoC2 injection compared with the plasma of pre-injection (week 0 [W0]) and AAV-GFP, in which plasma TG levels were completely normalized to those observed in WT animals (Figure 4B). The hApoC2 protein was also detectable in plasma at week 8 in animals treated with AAV-hApoC2, but not in those administered AAV-GFP (Figure 4C).

Furthermore, our study showed that intraperitoneal (i.p.) injection of AAV-hApoC2 was as effective as orbital vein injection with the same dose (2×10^{11} vg) in the prevention of neonatal death in ApoC2$^{-/-}$ pups. Plasma TG levels of pups administered AAV-hApoC2 via either the i.v. or i.p. route were markedly reduced in comparison to those of AAV-GFP-treated controls through the entire experimental period of 16 weeks (Figure 4D). It was shown that hApoC2 protein could be detected in plasma on day 7 (D7) after i.p. or orbital i.v. injection (Figure 4E). In the meantime, the abnormal plasma lipoprotein profile in ApoC2$^{-/-}$ pups with AAV-hApoC2 treatment was also completely corrected with a reduction in both TGs and cholesterol in the fractions of VLDL/CM and LDL, whereas cholesterol was elevated in the HDL group, which was similar to that observed in the WT group (Figures 4F and 4G).

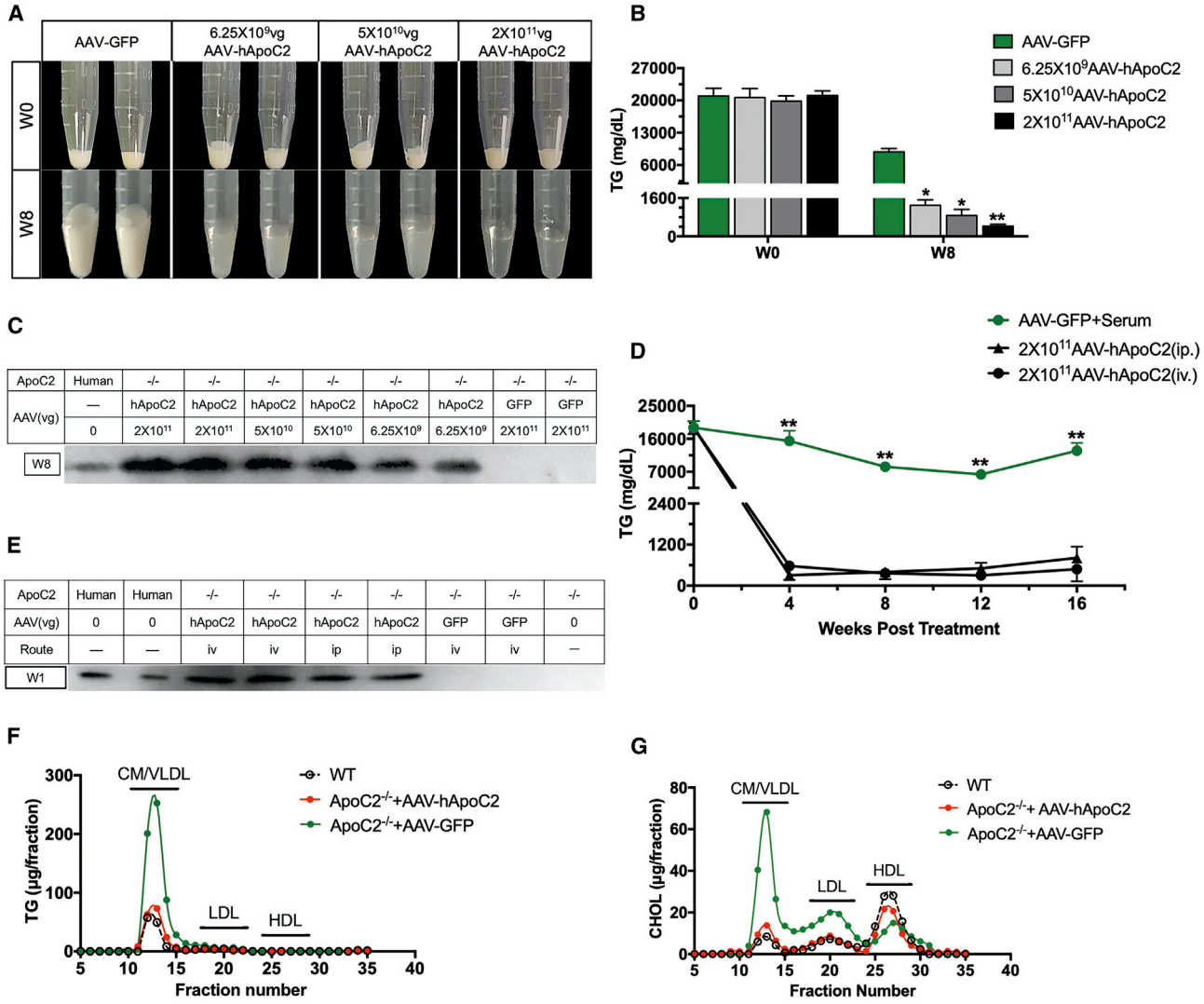

Figure 4. Effects of AAV-Mediated Human ApoC2 Expression on Plasma Lipids and Lipoproteins in Neonatal ApoC2$^{-/-}$ Hamsters

(A) Representative photos of plasma samples from neonatal ApoC2$^{-/-}$ hamsters before (W0) and 8 weeks (W8) after treatment with AAV-hApoC2 at three doses of 6.25 × 10^9, 5 × 10^{10}, and 2 × 10^{11} vg via orbital vein; the AAV-GFP-treated group at a dose of 2 × 10^{11} was used as control, in which concomitantly daily infusion of wild-type hamster serum via orbital vein was applied until weaning on day 21. (B) Analysis of plasma TG levels in animals from A. N = 3–4. *$p < 0.05$, **$p < 0.01$. (C) Representative western blots of plasma hApoC2 protein at W8 after administration of AAV-hApoC2 at three doses of 6.25 × 10^9, 5 × 10^{10}, and 2 × 10^{11} vg via orbital vein. (D) Time-course analysis of TG levels in AAV-GFP- or AAV-hApoC2-treated neonatal ApoC2$^{-/-}$ hamsters with a dose of 2 × 10^{11} vg injected via orbital vein (i.v.) or intraperitoneal (i.p.). N = 4–6 per group. **$p < 0.01$. (E) Representative western blots of plasma hApoC2 protein in neonatal ApoC2$^{-/-}$ hamsters at week 1 (W1) of AAV-hApoC2 at a dose of 2 × 10^{11} vg via intraperitoneal or orbital vein. (F) FPLC analysis of TG distribution from pooled plasma in WT, AAV-GFP-, and AAV-hApoC2-treated neonatal ApoC2$^{-/-}$ hamsters with a dose of 2 × 10^{11} vg at week 8. N = 6–8 per group. (G) FPLC analysis of cholesterol (CHOL) distribution from pooled plasma in WT, AAV-GFP-, and AAV-hApoC2-treated neonatal ApoC2$^{-/-}$ hamsters with a dose of 2 × 10^{11} vg at week 8. N = 6–8 per group.

AAV Treatment Had No Side Effects on Multiple Organ Damage

To investigate the side effects of AAV-mediated gene therapy in our study, we monitored liver and kidney function at the end of our experiments in each group with i.v. injection of AAV-hApoC2. As shown in Table 1, plasma alanine aminotransferase (ALT) and aspartate aminotransferase (AST) levels in both adult and neonatal ApoC2$^{-/-}$ hamsters with either AAV-hApoC2 or AAV-GFP were not significantly different from the WT control group without AAV administration, indicating clearly that AAV-hApoC2 did not cause significant liver damage or hepatotoxicity. Likewise, there were no significant differences in creatinine clearance (Ccr), 24-h urine protein, and blood urine nitrogen (BUN) among WT-, AAV-GFP-, and AAV-hApoC2-treated neonatal and adult ApoC2$^{-/-}$ hamsters, demonstrating no overt renal injury caused by AAV vectors to

Table 1. Liver and Kidney Function of Adult and Neonatal ApoC2$^{-/-}$ Hamsters after Treatment with AAV-hApoC2 and AAV-GFP

	WT	Adult + AAV-hApoC2	Newborn + AAV-hApoC2	Adult+ AAV-GFP
ALT activity (U/L)	20.75 ± 5.37	15.63 ± 1.76	15.67 ± 2.84	17.65 ± 8.94
AST activity (U/L)	18.62 ± 1.91	21.31 ± 4.41	16.68 ± 4.12	35.47 ± 3.19
Ccr (mL/min)	1.02 ± 0.06	0.83 ± 0.16	1.04 ± 0.13	0.73 ± 0.15
Urine protein/mg/24 h	1.44 ± 0.19	1.57 ± 0.62	1.3 ± 0.46	1.74 ± 0.32
BUN (mmol/L)	90.33 ± 23.4	104.1 ± 14.0	73.88 ± 8.75	116.8 ± 11.17

Wild-type (WT) hamsters and adult and neonatal ApoC2$^{-/-}$ hamsters were treated with AAV-hApoC2 (Adult + AAV-hApoC2, 2×10^{12} vg/hamster; Newborn + AAV, 2×10^{11} vg/pup) via jugular and orbital veins, respectively, Adult ApoC2$^{-/-}$ hamsters treated with AAV-GFP (Adult + AAV-GFP) via jugular vein were used as controls. ALT, alanine aminotransferase; AST, aspartate aminotransferase; Ccr, creatinin clearance; BUN, blood urine nitrogen. N = 4–5 per group. No statistical differences ($p > 0.05$) were detected among all four groups.

ApoC2$^{-/-}$ hamsters. Moreover, hematoxylin and eosin (H&E) staining of a variety of tissues at the end of the experiment showed that there were no apparent morphological changes in lung, kidney, and pancreas between AAV-GFP- and AAV-hApoC2-treated neonatal and adult ApoC2$^{-/-}$ hamsters, with both receiving high doses (2×10^{12} vg/adult hamster and 2×10^{11} vg/pup, respectively) (Figures 5A–5H), which is consistent with the results obtained from WT animals (Figure S1).

DISCUSSION

In this study, we used liver-specific AAV8 as a vector to establish long-term expression of the human *Apoc2* gene in ApoC2$^{-/-}$ hamsters. This means successfully corrected the sHTG in ApoC2$^{-/-}$ hamsters, and the lipid-lowering effect remained stable for up to 6 months. In the meantime, we also investigated the feasibility of this therapeutic modality in neonatal ApoC2$^{-/-}$ pups, given that familial ApoC2 deficiency often causes clinical phenomena such as abdominal pain due to acute pancreatitis during infancy and childhood. Although the route of i.p. injection in neonatal animals is simpler, the i.v. route should be preferable in view of similar gene therapy in human infants. The results obtained from neonatal hamsters showed that both i.p. and i.v. routes of AAV-hApoC2 completely corrected sHTG and then prevented neonatal death in newborn ApoC2$^{-/-}$ hamsters, which could survive to adulthood with a normal lipid profile due to the stable hApoC2 expression *in vivo*.

In the past decades, sHTG has been recognized as a disease with great concerns to clinicians due to the complication of recurrent and potentially life-threatening acute pancreatitis. However, because sHTG is primarily caused by different mutations in a single gene, it is possible that gene replacement therapy will achieve a good treatment goal. The first commercial gene therapy approved by the European Medicines Agency is applied for the treatment of sHTG caused by loss-of-function mutations in the *Lpl* gene.[23] Using AAV1 as a vector encoding a gain-of-function LPL mutant (LPLs447x, alipogene tiparvovec [Glybera]), which locally expresses LPL at the injection site after multiple intramuscular injections, can lower plasma TG levels to a certain extent in patients with *Lpl* null mutations in clinical trials, then leading to a reduction in the number of admissions to hospitals for acute pancreatitis.[24–27] Although Glybera has not been widely accepted due to the high cost and insurance issues, it has been shown that AAV gene therapy for sHTG is highly feasible in theory and practice.

Importantly, a critical issue to be considered in the development of gene therapy for sHTG is that FFAs generated from rapid hydrolysis of TGs may cause local tissue damage. This is why muscle was chosen as a target organ for Glybera gene therapy in the hope of avoiding the risk of liver toxicity induced by the abnormal accumulation of excessive FFAs from LPL-mediated TG hydrolysis. As expected, liver damage was not observed in early experimental gene therapy studies using adenoviruses as vectors for ectopic liver expression of LPL through i.v. injections.[28] However, although the quadriceps is adequately perfused, diffusion to neighboring muscle tissue through dozens of injection sites is bound to be limited. Therefore, a large number of AAV gene vectors can only be injected into the experimental animals to markedly reduce plasma TGs,[29,30] but in clinical trials, a high dose of AAV vectors was not allowed due to the potential toxicity, leading to an unsatisfied TG-lowering outcome in the patients, in which plasma TGs were still well above normal levels.[27]

Based on the property of ApoC2 and the advantages of the AAV vector in the field of gene therapy, in this study we proposed that liver would be an ideal organ for ApoC2 gene therapy because ApoC2 was largely synthesized by liver and then secreted into bloodstream, where it activated LPL anchored at the vascular endothelium for TG hydrolysis. Moreover, the high affinity of the AAV8 vector to the hepatocytes made cells to be efficiently infected by AAV-hApoC2 via the i.v. route, resulting in the exogenous hApoC2 expression at appropriate doses.[8,31,32] Our western blots showing high levels of hApoC2 in the plasma after administration of AAV-hApoC2 further supported this concept. Additionally, because hApoC2 is highly homologous to hamster ApoC2, it is logical that hApoC2 should be able to fully activate hamster LPL, thus effectively and rapidly ameliorating sHTG in ApoC2$^{-/-}$ hamsters.

Although our data suggest that AAV-hApoC2 could solve the problems caused by ApoC2 deficiency in hamsters, there are still some limitations in our current study. Previous studies have shown that overexpression of hApoC2 in transgenic mice caused the unexpected HTG because excess ApoC2 could disrupt the contact of

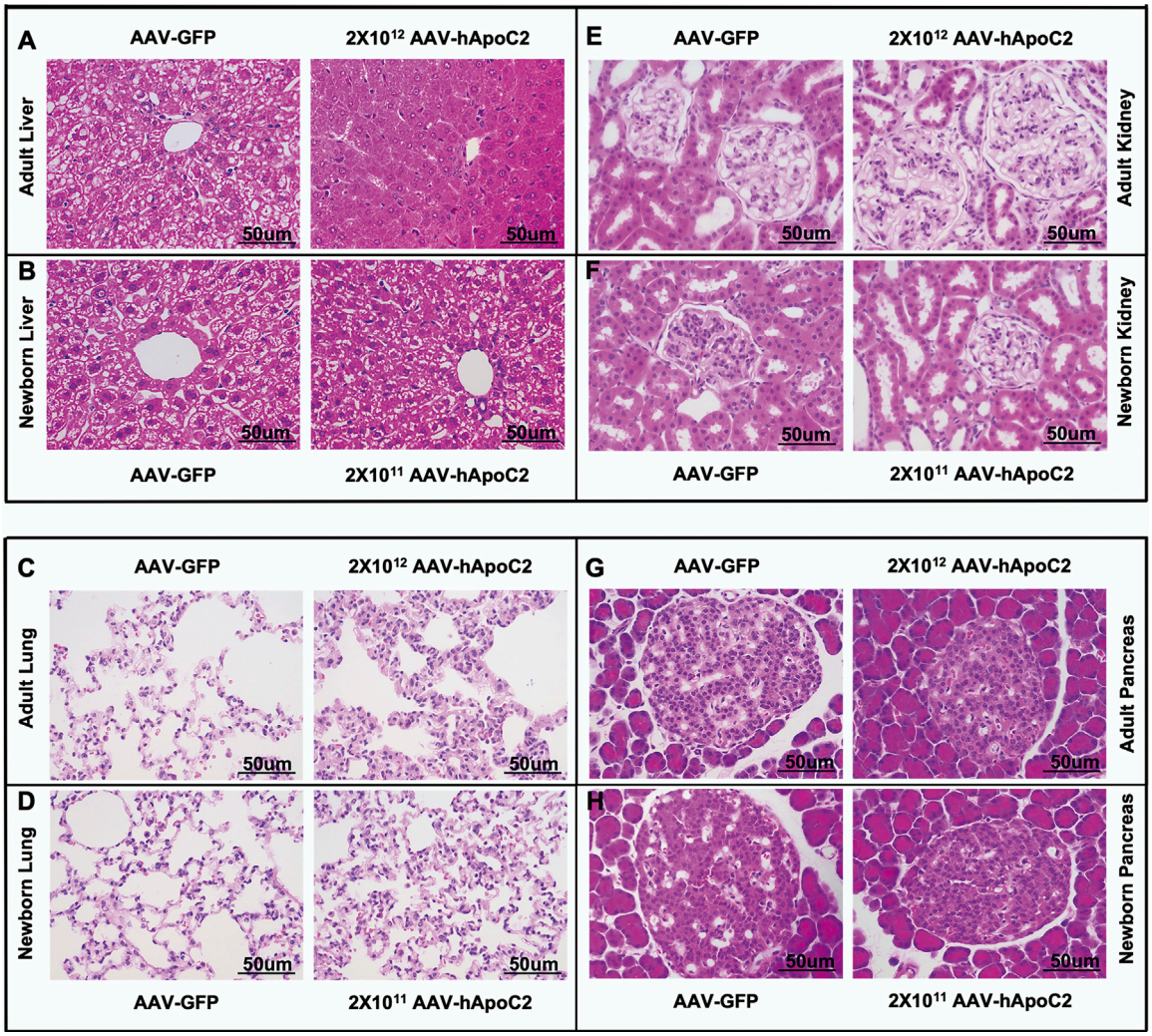

Figure 5. Morphological Analysis of Different Tissues in Adult and Neonatal ApoC2$^{-/-}$ Hamsters after Intravenous Administration of AAV-hApoC2

(A and B) Representative images for H&E staining of liver in adult (A) and neonatal (B) hamsters treated with AAV-hApoC2 or AAV-GFP intravenously at a dose of 2×10^{12} vg, respectively. (C and D) Representative images for H&E staining of lung from animals described in A (C) and B (D). (E and F) Representative images for H&E staining of kidney from animals described in A (E) and B (F). (G and H) Representative images for H&E staining of pancreas from animals described in A (G) and B (H). Scale bars, 50 μm.

TG-rich lipoprotein and LPL, indicating that TG metabolism mediated by the ApoC2/LPL complex is not fully understood.[33] It will be tempting for us to investigate the influence of hApoC2 overexpression on TG metabolism in WT hamsters in the future, which will help us understand whether ApoC2 gene therapy can be extrapolated to other forms of HTG caused by the mutations in TG metabolism-related genes, such as LPL, ANGPTLs, and GPIHBP1, but not ApoC2. Furthermore, we still do not know how long AAV-mediated hApoC2 expression will last based on our 6-month experiments at the current stage, suggesting that a longer time window should be studied.

In conclusion, we herein report for the first time that AAV8 vector encoding hApoC2 could be safely administered to both neonatal and adult ApoC2$^{-/-}$ hamsters to effectively reduce extremely high TG levels and prevent neonatal death secondary to sHTG in a long-term manner without any reverse effects on tissue damage. Our novel findings provide a new insight into the possibility that AAV8-mediated hepatic gene expression of hApoC2 will be a promising therapeutic approach for sHTG caused by ApoC2 deficiency.

MATERIALS AND METHODS

Construction of Viral Vectors

AAV8-hApoC2 was generated using a duplex AAV8 vector to carry a human *Apoc2* gene expression frame containing a target sequence of human miR-142-3p (Figure 6), which was provided by Beijing FivePlus Molecular Medicine Institute. The purpose of miR-142-3p insertion was to reduce the immunogenicity of the transgene product by

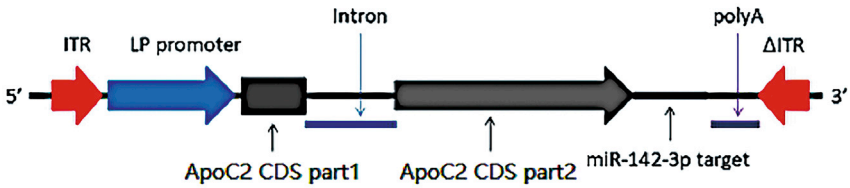

Figure 6. Structure Diagram of AAV Plasmid Vector AAV-hApoC2 Carrying the Human *Apoc2* Gene

inhibiting the translation of its target transcripts in antigen-presenting cells (APCs) and stabilize gene transfer.[34] The AAV8-hApoC2 construct has the following novel features: (1) the liver-specific LP15 promoter at upstream of the *Apoc2* gene for tissue-specific and effective expression;[35,36] (2) an optimized *Apoc2* coding region sequence with insertion of short introns for increased transcription efficiency;[37,38] (3) very low immunogenicity with an insertion of four target sequences of miR-142-3p in the 3′ UTR region;[34] and (4) a safe and non-pathogenic recombinant double-stranded AAV8 vector.[39]

Animals

ApoC2$^{-/-}$ hamsters were created in our laboratory as described previously,[18] which showed the characteristics of sHTG and death during the lactation period. Because all neonatal ApoC2$^{-/-}$ hamsters died within 10 days after birth, daily administration of normal hamster serum via the orbital vein was needed for rescue until weaning on day 21. Neonatal or adult ApoC2$^{-/-}$ animals rescued from neonatal death by normal hamster serum were used for the future experiments. The animals were housed under humidity of 50%–60% at 22°C–24°C on a 14-h light/10-h dark cycle with water *ad libitum*. The experimental procedures for animals were strictly in accordance with NIH requirements (NIH released no. 85Y231996 revision) and approved by the Ethics Committee of Laboratory Animals of Peking University (LA2010-059). Isoflurane inhalation was used as the anesthetic method for experimental animals.

AAV-hApoC2 Experiments

Neonatal ApoC2$^{-/-}$ Hamsters

On postnatal day 3, neonatal ApoC2$^{-/-}$ pups were injected with AAV-hApoC2 via orbital vein (i.v.) or i.p., and neonatal ApoC2$^{-/-}$ hamsters receiving AAV-GFP as controls were also given i.v. infusion of normal hamster serum until weaning to ensure survival. All vector doses were per pup, and the average weight was 3 g. The animals were sacrificed at week 8 after treatment, and the related tissues were taken for assessment of relevant gene expression and morphological evaluation.

Adult ApoC2$^{-/-}$ Hamsters

Adult ApoC2$^{-/-}$ hamsters were injected with AAV-hApoC2 via the external jugular vein at a dose of virus per animal. Blood was collected from the pups and adult hamsters through the femoral artery and jugular vein, respectively, at the indicated time points for the determination of serum lipids and ApoC2 protein. The animals were sacrificed at week 12 after treatment and the tissues were harvested for measurement of gene expression and morphological evaluation.

Rescue of ApoC2$^{-/-}$ Hamsters

ApoC2-containing serum from WT hamsters was used to rescue the lethality of ApoC2$^{-/-}$ pups during the lactation period. Briefly, blood was collected from WT hamsters via the retro-orbital veins and incubated at 37°C for 30 min, followed by a centrifugation at 4,000 rpm for 10 min at room temperature. Supernatants were collected and then filtered through a 0.22-μm syringe filter (Millipore, USA) and stored at −20°C for further experiments. We injected normal hamster serum into ApoC2$^{-/-}$ pups through the retro-orbital route on day 3 after birth at a single dose of 10 μL per gram of body weight daily until weaning on day 21.

Plasma Lipids and Lipoproteins

Plasma TC and TG levels were measured by the enzymatic method (Biosino Bio Technology & Science, Beijing, China). Plasma hApoC2 was detected by western blots. Briefly, 3 μL of plasma was mixed with a buffer containing sodium lauryl sulfate (SDS) and dithiothreitol (DTT), boiled at 95°C for 10 min, and then loaded onto 15% SDS-PAGE gels. The hApoC2 protein was visualized using rabbit against hApoC2 (ab76452, Abcam, Cambridge, UK, rabbit polyclonal immunoglobulin G [IgG], 1:1,000).

Lipoprotein analysis was performed by FPLC on a Superose 6 HR10/30 column (Amersham Biocsciences, USA). The 200-μL pooled plasma samples from indicated groups were first treated by ultracentrifugation at 25,000 rpm for 15 min to get rid of the extremely large lipoprotein particles in order to prevent the obstruction of the column, then filtered through a 0.22-μm syringe filter (Millipore, USA). The fractions were eluted at a rate of 0.5 mL per min with PBS and automatically collected. A total of 35 fractions with 500 μL were used to determine TC and TGs in each fraction.

RNA Extraction and Quantitative Real-Time PCR

Total RNA was extracted with TRIzol reagent (Invitrogen, USA), and the first-strand cDNA was generated with a reverse transcription (RT) kit (Promega, USA). Quantitative real-time PCR was performed to measure gene expression using different pairs of primers (Table S1). Quantitative real-time PCR was conducted using an Applied Biosystems with SYBR Green fluorescence (Promega, USA) for 40 cycles, which consisted of heat denaturation at 95°C for 30 s and annealing extension at 60°C for 60 s. All relative gene expression levels were normalized to GAPDH.

Liver and Kidney Function

Serum ALT, AST, and creatinine in the indicated groups were measured according to the instructions of commercial kits (Nanjing

Jiancheng Co., China, and R&D Systems, USA). A metabolic cage (Tecniplast, Italy) was applied to collect 24-h urine samples for the measurement of creatinine (R&D Systems, USA) and albumin (Bethyl Laboratories, USA). Blood urea nitrogen was assayed using a commercial kit (Nanjing Jiancheng).

Morphological Analysis

Animals were sacrificed at the indicated time points and perfused with 20 mL of 0.01 M PBS through the left ventricle. Tissues of liver, kidney, lung, and pancreas were harvested, fixed with 4% paraformaldehyde, and then embedded in paraffin. Sections (5 μm) were stained with H&E. Briefly, the samples were incubated with xylene and ethanol to remove paraffin, stained for 5 min with hematoxylin, followed by incubation with eosin for 3 min. Then, the sections were re-immersed in ethanol and xylene and observed under microscope.

Statistical Analysis

All experimental data are presented as mean ± standard error. Statistical analysis was performed using Student's t test or one-way variance (ANOVA) followed by Tukey's posterior test using GraphPad Prism 7.0. p values less than 0.05 were considered statistically significant.

SUPPLEMENTAL INFORMATION

Supplemental Information can be found online at https://doi.org/10.1016/j.omtm.2020.07.011.

AUTHOR CONTRIBUTIONS

Conceptualization, G.L. and X.X.; Methodology, G.L., X.X., and C.Y.; Investigation, C.Y., M.G (Mengmeng Guo)., and F.G.; Validation, C.Y. and X.L., Formal Analysis, C.Y.; Resources, W.T., S.M., and X.D.; Writing – Original Draft, C.Y.; Writing – Review & Editing, G.L. and X.X.; Funding Acquisition, M.G (Mingming Gao)., Y.W. X.X., and G.L.; Supervision, G.L. and X.X.

CONFLICTS OF INTEREST

The authors declare no competing interests.

ACKNOWLEDGMENTS

This work was supported by the following grants: NSFC 31520103909 and 81270367 (to G.L.); NSFC 31771306 and 81700386 (to M.G.); BMU2020MX001 (to X.X.); and National Key Research and Development Program of China (2016YFE0126000) (to Y.W.). G.L. is a fellow at the Collaborative Innovation Center for Cardiovascular Disease Translational Medicine, Nanjing Medical University.

REFERENCES

1. Kersten, S. (2014). Physiological regulation of lipoprotein lipase. Biochim. Biophys. Acta *1841*, 919–933.
2. Chait, A., and Subramanian, S. (2000). Hypertriglyceridemia: pathophysiology, role of genetics, consequences, and treatment. In Endotext (MDText.com), https://www.ncbi.nlm.nih.gov/books/NBK326743/.
3. Goldberg, I.J., Scheraldi, C.A., Yacoub, L.K., Saxena, U., and Bisgaier, C.L. (1990). Lipoprotein ApoC-II activation of lipoprotein lipase. Modulation by apolipoprotein A-IV. J. Biol. Chem. *265*, 4266–4272.
4. Ueda, M., Dunbar, R.L., Wolska, A., Sikora, T.U., Escobar, M.D.R., Seliktar, N., deGoma, E., DerOhannessian, S., Morrell, L., McIntyre, A.D., et al. (2017). A novel APOC2 missense mutation causing apolipoprotein C-II deficiency with severe triglyceridemia and pancreatitis. J. Clin. Endocrinol. Metab. *102*, 1454–1457.
5. Wang, H., and Eckel, R.H. (2009). Lipoprotein lipase: from gene to obesity. Am. J. Physiol. Endocrinol. Metab. *297*, E271–E288.
6. Palacio Rojas, M., Prieto, C., Bermúdez, V., Garicano, C., Núñez Nava, T., Martínez, M.S., Salazar, J., Rojas, E., Pérez, A., Marca Vicuña, P., et al. (2017). Dyslipidemia: genetics, lipoprotein lipase and HindIII polymorphism. F1000Res. *6*, 2073.
7. Brahm, A.J., and Hegele, R.A. (2015). Chylomicronaemia—current diagnosis and future therapies. Nat. Rev. Endocrinol. *11*, 352–362.
8. Wolska, A., Dunbar, R.L., Freeman, L.A., Ueda, M., Amar, M.J., Sviridov, D.O., et al. (2017). Apolipoprotein C-II: new findings related to genetics, biochemistry, and role in triglyceride metabolism. Atherosclerosis. *267*, 49–60.
9. Gelrud, A., Williams, K.R., Hsieh, A., Gwosdow, A.R., Gilstrap, A., and Brown, A. (2017). The burden of familial chylomicronemia syndrome from the patients' perspective. Expert Rev. Cardiovasc. Ther. *15*, 879–887.
10. Davidson, M., Stevenson, M., Hsieh, A., Ahmad, Z., Crowson, C., and Witztum, J.L. (2017). The burden of familial chylomicronemia syndrome: interim results from the IN-FOCUS study. Expert Rev. Cardiovasc. Ther. *15*, 415–423.
11. Davidson, M., Stevenson, M., Hsieh, A., Ahmad, Z., Roeters van Lennep, J., Crowson, C., and Witztum, J.L. (2018). The burden of familial chylomicronemia syndrome: results from the global IN-FOCUS study. J. Clin. Lipidol. *12*, 898–907.e2.
12. Jiang, J., Wang, Y., Ling, Y., Kayoumu, A., Liu, G., and Gao, X. (2016). A novel APOC2 gene mutation identified in a Chinese patient with severe hypertriglyceridemia and recurrent pancreatitis. Lipids Health Dis. *15*, 12.
13. Chen, T.Z., Xie, S.L., Jin, R., and Huang, Z.M. (2014). A novel lipoprotein lipase gene missense mutation in Chinese patients with severe hypertriglyceridemia and pancreatitis. Lipids Health Dis. *13*, 52.
14. Sakurai, T., Sakurai, A., Vaisman, B.L., Amar, M.J., Liu, C., Gordon, S.M., Drake, S.K., Pryor, M., Sampson, M.L., Yang, L., et al. (2016). Creation of apolipoprotein C-II (ApoC-II) mutant mice and correction of their hypertriglyceridemia with an ApoC-II mimetic peptide. J. Pharmacol. Exp. Ther. *356*, 341–353.
15. Liu, C., Gates, K.P., Fang, L., Amar, M.J., Schneider, D.A., Geng, H., Huang, W., Kim, J., Pattison, J., Zhang, J., et al. (2015). Apoc2 loss-of-function zebrafish mutant as a genetic model of hyperlipidemia. Dis. Model. Mech. *8*, 989–998.
16. Dong, Z., Shi, H., Zhao, M., Zhang, X., Huang, W., Wang, Y., et al. (2018). Loss of LCAT activity in the golden Syrian hamster elicits pro-atherogenic dyslipidemia and enhanced atherosclerosis. Metabolism. *83*, 245–255.
17. Guo, X., Gao, M., Wang, Y., Lin, X., Yang, L., Cong, N., et al. (2018). LDL receptor gene-ablated hamsters: a rodent model of familial hypercholesterolemia with dominant inheritance and diet-induced coronary atherosclerosis. EBioMedicine. *27*, 214–224.
18. Gao, M., Yang, C., Wang, X., Guo, M., Yang, L., Gao, S., et al. (2020). ApoC2 deficiency elicits severe hypertriglyceridemia and spontaneous atherosclerosis: A rodent model rescued from neonatal death. Metabolism. *109*, 154296.
19. Breckenridge, W.C., Little, J.A., Steiner, G., Chow, A., and Poapst, M. (1978). Hypertriglyceridemia associated with deficiency of apolipoprotein C-II. N. Engl. J. Med. *298*, 1265–1273.
20. Naso, M.F., Tomkowicz, B., Perry, W.L., 3rd, and Strohl, W.R. (2017). Adeno-associated virus (AAV) as a vector for gene therapy. BioDrugs. *31*, 317–334.
21. Colella, P., Ronzitti, G., and Mingozzi, F. (2017). Emerging issues in AAV-mediated *in vivo* gene therapy. Mol. Ther. Methods Clin. Dev. *8*, 87–104.
22. Berns, K.I., and Muzyczka, N. (2017). AAV: an overview of unanswered questions. Hum. Gene Ther. *28*, 308–313.
23. Ylä-Herttuala, S. (2012). Endgame: Glybera finally recommended for approval as the first gene therapy drug in the European Union. Mol. Ther. *20*, 1831–1832.
24. Miller, N. (2012). Glybera and the future of gene therapy in the European Union. Nat. Rev. Drug Discov. *11*, 419.
25. Carpentier, A.C., Frisch, F., Labbé, S.M., Gagnon, R., de Wal, J., Greentree, S., Petry, H., Twisk, J., Brisson, D., and Gaudet, D. (2012). Effect of alipogene tiparvovec

(AAV1-LPL^{S447X}) on postprandial chylomicron metabolism in lipoprotein lipase-deficient patients. J. Clin. Endocrinol. Metab. *97*, 1635–1644.

26. Gaudet, D., Brisson, D., Methot, J., and Deventer, S.V. (2009). An open-label, dose escalation study to assess the safety and efficacy of AAV1-LPL S447X gene therapy with alipogene tiparvovec (AMT-011) for patients with severe hypertriglyceridemia due to lipoprotein lipase deficiency (LPLD). Atheroscler. Suppl. *10*, e286.

27. Gaudet, D., Méthot, J., Déry, S., Brisson, D., Essiembre, C., Tremblay, G., Tremblay, K., de Wal, J., Twisk, J., van den Bulk, N., et al. (2013). Efficacy and long-term safety of alipogene tiparvovec (AAV1-LPL^{S447X}) gene therapy for lipoprotein lipase deficiency: an open-label trial. Gene Ther. *20*, 361–369.

28. Excoffon, K.J.D.A., Liu, G., Miao, L., Wilson, J.E., McManus, B.M., Semenkovich, C.F., Coleman, T., Benoit, P., Duverger, N., Branellec, D., et al. (1997). Correction of hypertriglyceridemia and impaired fat tolerance in lipoprotein lipase-deficient mice by adenovirus-mediated expression of human lipoprotein lipase. Arterioscler. Thromb. Vasc. Biol. *17*, 2532–2539.

29. Ross, C.J.D., Twisk, J., Meulenberg, J.M., Liu, G., van den Oever, K., Moraal, E., Hermens, W.T., Rip, J., Kastelein, J.J., Kuivenhoven, J.A., and Hayden, M.R. (2004). Long-term correction of murine lipoprotein lipase deficiency with AAV1-mediated gene transfer of the naturally occurring LPL^{S447X} beneficial mutation. Hum. Gene Ther. *15*, 906–919.

30. Ross, C.J.D., Twisk, J., Kuivenhoven, J.A., Liu, G., Miao, F., Oever, K.V.D., Beetz, M., Verbart, D., Bakker, A., Oranje, P.P.A., et al. (2004). Correction of dyslipidemia in murine and feline models of lipoprotein lipase deficiency by intramuscular administration of AAV1-LPL^{S447X}. Mol. Ther. *9* (*Suppl 1*), S17.

31. Datta, S., Li, W.H., Ghosh, I., Luo, C.C., and Chan, L. (1987). Structure and expression of dog apolipoprotein C-II and C-III mRNAs. Implications for the evolution and functional constraints of apolipoprotein structure. J. Biol. Chem. *262*, 10588–10593.

32. Fojo, S.S., Taam, L., Fairwell, T., Ronan, R., Bishop, C., Meng, M.S., Hoeg, J.M., Sprecher, D.L., and Brewer, H.B., Jr. (1986). Human preproapolipoprotein C-II. Analysis of major plasma isoforms. J. Biol. Chem. *261*, 9591–9594.

33. Shachter, N.S., Hayek, T., Leff, T., Smith, J.D., Rosenberg, D.W., Walsh, A., Ramakrishnan, R., Goldberg, I.J., Ginsberg, H.N., and Breslow, J.L. (1994). Overexpression of apolipoprotein CII causes hypertriglyceridemia in transgenic mice. J. Clin. Invest. *93*, 1683–1690.

34. Majowicz, A., Maczuga, P., Kwikkers, K.L., van der Marel, S., van Logtenstein, R., Petry, H., van Deventer, S.J., Konstantinova, P., and Ferreira, V. (2013). Mir-142-3p target sequences reduce transgene-directed immunogenicity following intramuscular adeno-associated virus 1 vector-mediated gene delivery. J. Gene Med. *15*, 219–232.

35. Rouet, P., Raguenez, G., Tronche, F., Yaniv, M., N'Guyen, C., and Salier, J.P. (1992). A potent enhancer made of clustered liver-specific elements in the transcription control sequences of human alpha 1-microglobulin/bikunin gene. J. Biol. Chem. *267*, 20765–20773.

36. Urano, Y., Watanabe, K., Sakai, M., and Tamaoki, T. (1986). The human albumin gene. Characterization of the 5′ and 3′ flanking regions and the polymorphic gene transcripts. J. Biol. Chem. *261*, 3244–3251.

37. Kim, C.H., Oh, Y., and Lee, T.H. (1997). Codon optimization for high-level expression of human erythropoietin (EPO) in mammalian cells. Gene. *199*, 293–301.

38. Shaul, O. (2017). How introns enhance gene expression. Int. J. Biochem. Cell Biol. *91* (Pt B), 145–155.

39. Markusic, D.M., and Herzog, R.W. (2012). Liver-directed adeno-associated viral gene therapy for hemophilia. J. Genet. Syndr. Gene Ther. *1*, 1–9.